Received: Added at production | Revised: Added at production | Accepted: Added at production

DOI: xxx/xxxx

RESEARCH

Priming of retrograde signaling in wheat across multiple natural environments reveal how responses to dynamic stimuli can be integrated to alter yield, yield stability and water productivity

Andrew F. Bowerman[1,4] | Marten Moore[1,4] | Arun Yadav[1,4,5] | Jing Zhang[1] | Matthew D. Mortimer[1] | Zuzana Plšková[1] | Estee E. Tee[1,2] | Eng Kee Au[1] | Derek P. Collinge[1] | Gonzalo M. Estavillo[1,3] | Crispin A. Howitt[3] | Kai X. Chan[1] | Greg J. Rebetzke[3] | Barry J. Pogson[1,5]

[1]Research School of Biology, The Australian National University, Canberra, 2601, ACT, Australia

[2]The John Innes Centre, Norwich Research Park, Norwich, NR4 7UH, United Kingdom

[3]CSIRO Agriculture and Food, Canberra, 2601, ACT, Australia

[4]AFB, MM and AY contributed equally to this work

[5]Corresponding Authors

Correspondence
Corresponding authors Barry J. Pogson and Arun Yadav.
Email: barry.pogson@anu.edu.au
arunkumar102@gmail.com

Summary

• Chloroplasts act as environmental sensors, enabling rapid plant stress responses through operational retrograde signaling. While these signals operate on minutes-to-hours' time scales, their cumulative impact and function across a plant's lifecycle and in field conditions remains unknown.
• We investigated if retrograde signaling's transient changes to gene expression have cumulative effects by generating wheat mutants with primed SAL1-PAP retrograde pathway responsiveness. After confirming changes in photosynthesis and drought resilience under controlled conditions, we conducted 15 field trials across South-Eastern Australia, spanning diverse environments with varying temperatures, rainfall, and light conditions, analysing physiological responses, yield, biomass, and water productivity.
• We found gene locus-specific effects on biomass, yield, and water productivity. Multi-environment analysis showed the SAL-4A locus was more strongly associated with improved performance, with the converse for SAL-5D. Significantly, modulation of specific SAL subtypes enhanced photosynthetic efficiency and stress resilience while improving average yields by 4 and 8% respectively for 4A loci across 15 field sites, challenging the traditional yield-resilience trade-off paradigm.
• This study reveals retrograde signals operate in field environments, integrating environmental information across a plant's lifecycle to improve yield, water productivity and dynamic acclimation to diverse growing seasons, and highlight the importance of multi-environment field validation for crop modifications.

KEYWORDS
Drought | Retrograde signaling | Wheat | Chloroplast | Photosynthesis | SAL1

INTRODUCTION

Climate variability poses an escalating threat to global food security, demanding urgent advances in crop stress tolerance (Bowerman et al. 2023). Modern crops face an unprecedented combination of abiotic stresses - from extreme temperatures and water availability to excess light and nutrient imbalances - often occurring simultaneously or in rapid succession. Plants coordinate their responses to these challenges through intricate cellular signaling networks, where even subtle changes in key pathways can trigger extensive transcriptional and physiological adaptations. Among these networks, chloroplast-to-nucleus retrograde signaling plays a particularly crucial role in integrating environmental cues with cellular responses (for review, see Pogson et al. (2008), Chan et al. (2016b), Crawford et al. (2018), Calderon and Strand (2021)). These signals are essential for coordinating cellular responses to transient stress, and for optimal plastid operation given the number of plastid-located protein complexes that are nuclear encoded and subject to damage by oxidative stress. (Jan et al. 2022).

Abbreviations: PAP, 3'-phosphoadenosine 5'-phosphate

 © 2025 Copyright Holder Name

The SAL1 enzyme, an adenosine phosphatase (EC:3.1.3.7), regulates the levels of 3'-phosphoadenosine 5'-phosphate (PAP), a chloroplast-to-nucleus signal molecule (for review, see Jan et al. (2022)). SAL1 converts PAP into adenosine monophosphate (AMP), and is a negative regulator of excess light and drought tolerance in *Arabidopsis thaliana*. Under drought or light stress, SAL1 becomes inactivated by oxidation, allowing PAP to accumulate and move between organelles, increasing up to 30-fold in *Arabidopsis* (Estavillo et al. 2011, Chan et al. 2016a). Elevated PAP affects the expression of a raft of genes, partly through inhibition of exoribonucleases (XRNs) and resulting promotion of RNA polymerase II read-through at transcription termination sites (Estavillo et al. 2011, Gigolashvili et al. 2012, Crisp et al. 2018, Ashykhmina et al. 2019).

Studies of retrograde signaling in general (and SAL1 in particular) have largely focused on gene knockout lines in model species. Without a functional SAL1 protein, such knockouts constitutively accumulate PAP to high levels without stress induction, approximately 20-fold in *Arabidopsis alx8* mutants (Estavillo et al. 2011). These lines exhibit increased drought stress tolerance (40-50% longer survival compared to wild type) and improved water use efficiency with a decreased growth rate, dwarf phenotype, and leaf morphology changes (Rossel et al. 2006, Wilson et al. 2009). PAP itself has been implicated directly in the control of stomatal aperture closure across diverse taxa with functioning stomata, from mosses and ferns to monocots and dicots (Zhao et al. 2019). PAP bypasses and augments canonical ABA signaling; this includes exogenous and endogenous addition of PAP to ABA-insensitive *Arabidopsis* lines restoring stomatal closure (Pornsiriwong et al. 2017). Broader effects of knocking out SAL1 include changes in hormone levels, induction of phosphate starvation responsive gene expression, and modified metabolome including altered levels of osmoprotective compounds (Rossel et al. 2006, Wilson et al. 2009, Hirsch et al. 2011). Thus, determining the transient stress-responsive functions of PAP *bona fide* is confounded by the persistently elevated concentrations of PAP in mutants, which result in developmental anomalies (Phua et al. 2018a).

Recent studies in wheat (*Triticum aestivum L.*), which possesses a more complex SAL gene family than Arabidopsis, show varied outcomes from attempts to knock down all SAL1 copies simultaneously, including purported yield penalties alongside improved resilience. VIGS-mediated silencing improved drought tolerance markers (Manmathan et al. 2013), while CRISPR-based knockouts reported enhanced stress resistance based on osmotic shock experiments (Abdallah et al. 2022) and yield penalties in pots subject to competitive glasshouse conditions (Mohr et al. 2022); noting that pot-based yields are perilous measures (Passioura 2006). None of these studies considered the roles of different SAL homeoforms, assayed any traits in the field, or measured the impacts of the genetic modification on the enzyme (SAL1) and its substrate (PAP). Nor did they consider whether retrograde signaling is a transient process or is integrated across the life cycle.

Indeed, more broadly retrograde signaling research has focused on standardized conditions with single stresses, rather than the complex, unpredictable stress combinations crops face in the field, and ignored if it has a cumulative effect on the entire life cycle of plants in response to multifactorial stresses (for review of multifactorial stress, see Zandalinas and Mittler (2022)). The SAL1-PAP pathway's role in coordinating chloroplast stress response, regulating hormonal signaling, and metabolic responses makes it ideal for studying these complex conditions (Phua et al. 2018b). However, this necessitates a different strategy to simple loss-of-function genetic modifications and single stresses in controlled environments.

The challenges we meet in this report are to first test the null hypothesis that short-term changes mediated by retrograde signaling pathways have no ongoing impact on crops grown in dynamic and varied environments. Second, to consider how do we best translate findings in a model plant under controlled environments into crops that are selected for high and stable yields across multiple environments? Our strategy was to create knockouts of select SAL1 homeologues in wheat. SAL is typically in excess (Chan et al. 2016a), which means that PAP levels remain low unless the stress is significant (Phua et al. 2018a). By reducing one to two of the six homeologues present in cv. Chara, we engineered plants with diminished overall SAL activity, thereby necessitating less stress to induce PAP. We postulate that such primed plants would respond more dynamically to environmental perturbations. We utilized heavy ion bombardment (HIB) to knockout *TaSAL* genes, enabling us to assess these materials in natural environments during a period when gene-edited field trials were not authorized (2015-2019) and producing a crop that is globally far more deployable to industry. Our evaluation of the primed retrograde signaling plants in natural environments was conducted across 15 distinct settings, covering four different cereal-growing districts over five years, characterized by varying rainfall and irrigation regimes. Subsequently, we incorporated the observations into a multi-environment trial (MET) model to examine whether modulation of retrograde signaling influences altered lifetime responses to diverse and dynamic natural environments. An additional aspect of the study involves an evaluation of the trade-offs in yield resilience for genes that can modulate both stress responses and developmental processes.

MATERIALS AND METHODS

Phylogeny and expression analysis

Sequence homologues of AtSAL1 (NP_201203.3) were identified from Liliopsida using Uniprot BLAST (e-value < 0.1). A sequence similarity network was constructed and filtered to retain sequences with $\geq$ 40% identity that clustered with Arabidopsis SAL1/2/3/4 references, and sequences between 250-600 amino acids in length. Wheat sequences were updated using homologues identified from Gramene, and AHL enzyme sequences were added as an out-group. Multiple sequence alignment was performed using T-COFFEE, refined with MAFFT, and manually curated. Sequences with non-consensus insertions/deletions were removed. Phylogenetic reconstruction used ModelFinder for model selection, with multiple replicates and ultrafast bootstraps. The final

phylogeny was selected based on outgroup contiguity and visualized in R. Detailed protocols and software versions are provided in Supporting Methods S1.

Expression data were retrieved from the Wheat RNA-seq Database https://plantrnadb.com/wheatrna/ (Zhang et al. 2020) and from the database of Loudya et al. (2021). Gene co-expression analysis was performed using ATTED-II, using all members of each TaSAL group as seed sequences. The top 100 co-expressed genes for TaSAL1 and TaSAL2 were then used in ShinyGo v0.80 to summarise GO terms related to these co-expressed genes (Ge et al. 2020).

Identification of *TaSAL1* mutants and generation of double null lines

A wheat population mutagenised by heavy ion bombardment (HIB) was used to search for mutations in each *TaSAL1* homeologues (Regina et al. 2015). Rather than single nucleotide changes which are seen in chemical mutation-based populations, HIB mutations result in large deletion mutations, usually encompassing entire genes. A total of 3000 individual M3 HIB lines were screened using homeoform specific primers for deletions in each *TaSAL1* gene by PCR, resulting in the identification of five primary null lines, three deletions on chromosome 4A and two on chromosome 5D. Primer sequences are listed in Supporting Information Table S1. Multiple crosses were generated using combinations of each of these null lines; all line details are found in Supporting Information Table S2. Deletions were characterised using two targeted genotype-by-sequencing (tGBS) approaches, completed by Agriculture Victoria (AgriBio, Bundoora, Australia). Briefly, one tGBS assay was constructed from a subset of the Infinium 90K SNP chip (Chidzanga et al. 2021), and the second tGBS method was constructed using exome sequencing results from approx. 1000 wheat lines (Sharma et al. 2022). Combined, this maximised the marker density and maximised our chances of identifying deletions. See Supporting Information Table S1 for details of primer sequences and lines identified by this process, and details of deletion characterisation are found in the Supplementary Files.

Plant growth and drought stress in glasshouse

All lines were grown in a controlled greenhouse with day-length extension to 16h at 24/16 °C day/night temperature and 60% relative humidity. Pots of 25 cm (diameter) × 30 cm (h) were filled with compost-based potting mix and arranged in a randomised complete block design. All pots were watered daily to pot capacity until drought stress was imposed at the 3-4 leaf stage (21 days). Two drought regimes were used. **Cyclic Drought**: At day 0 of drought, water was withheld in droughted plants until day 15 of the first drought and then re-watered to their 100% soil water capacity as per Bowne et al. (2012). Droughted plants were then subjected to a second drought by withholding water for a further 13 days, totalling 28 days. **Terminal drought**: All pots were saturated with water at day 0 and designated drought-stressed plants were not watered up to 42 days of drought. All control plants were maintained at 100% water capacity.

Field trial management

Performance of genotypes was assessed under a series of field trials undertaken across four seasons at four managed environment facilities in New South Wales, Australia. Details of facilities can be found in Rebetzke et al. (2013), and are indicated, along with temperature and rainfall variation between and within sites in Figure 4. Multiple trials were performed in each site/year with varying access to irrigation to ensure variation in water availability between trials. All designs were produced using a complete randomised block design approach. In all experiments, all the plots were treated with 30 mm of pre-sowing irrigation and entries were sown at an optimal 3 to 5 cm sowing depth into 6-m long, 0.17-m spaced, 8-row plots at seeding rates consistent with local practice (i.e. 120 seeds per m^2 at Narrabri, and 180 seeds per m^2 at Yanco and Condobolin). Where irrigation was supplied, it was calculated at the site to target 25% above mean rainfall. Nutrients were supplied at sowing as Starter 15® (14% N: 12.7% P: 11% S) applied at 103 $kg.ha^{-1}$. Additional nitrogen was applied as needed to meet crop demand. Plots were end-trimmed to 5.4 m length and border rows removed prior to machine harvesting for plot yield estimates.

PAP quantification, SAL1 activity assay and protein quantification

PAP was quantified using a modified version from Ashykhmina et al. (2019). Metabolites were extracted from liquid nitrogen-frozen leaf tissue (30-50 mg) using chloroform:methanol and citrate-phosphate buffer extraction. PAP was quantified by HPLC following chloracetaldehyde derivatization using commercial PAP as standard (Sigma-Aldrich, A5763). Separation was performed on a Kinetex XB-C18 column (Phenomenex) using tetrabutylammonium hydrogensulfate and acetonitrile buffers. Detailed protocols are provided in Supporting Method S2.

ABA quantification

Leaf ABA was quantified using a modified extraction protocol. Approximately 100 mg of flash-frozen leaf tissue was homogenized in a Tissue Lyser II (Qiagen, Germany) with a steel ball bearing at 19.5 Hz for 2 minutes. The tissue was extracted twice with 2 mL cold 80% methanol by overnight shaking (25 rpm, 4°C) followed by centrifugation (14,000 rpm, 4°C). After each extraction, supernatants were vacuum concentrated to 500 μL using a miVac Duo Concentrator (GeneVac, UK). A final methanol wash step was performed and concentrated to 500 μL. Combined concentrated extracts (1.5 mL total) were further reduced to 500 μL under vacuum. Extracts were acidified to pH 2.5 with 0.5 mM HCl and partitioned against equal volumes of ethyl acetate. The

organic phase was dried under vacuum and resuspended in 1 mL Tris-Buffered Saline (TBS). ABA was quantified using the Phytodetek ABA Kit (Agdia Inc, USA) according to manufacturer's instructions, with absorbance measured at 405 nm (Tecan Group, Switzerland). Final ABA concentrations were expressed as ng/g dry weight.

Photosynthesis, stomatal conductance, relative water content and carbon isotope discrimination

An open gas-exchange system with a 2x3 cm clamp-on leaf cuvette was used to simultaneously measure stomatal conductance and photosynthesis (Li-6400; Li-Cor, Inc., Lincoln, USA). The topmost expanded leaf was chosen for taking measurements. Measurements were taken after leaves were adapted in the chamber for approximately 10 minutes at 380 μmol CO_2 and light intensity of 1000 μmol/m/s, block temperature of 24°C, and ambient humidity approximately at 55%.

Relative water content was measured as in Wilson et al. (2009), with leaf sections cut and weighed to measure fresh weight (F_W). Leaves were incubated in water at 4°C in dark conditions, blotted, and reweighed to measure turgid weight (T_W). Finally, leaves were dried at 80°C overnight, weighed to determine dry weight (D_W), and relative water content was calculated as

$$RWC = \frac{F_W - D_W}{T_W - D_W}$$

Samples of dried and ground plant material were weighed to 1.5 mg (within 0.2 mg) into folded tin foil cups. These were then combusted in a Carlo-Erba EA-1110 Elemental Analyser (Carlo Erba, Milan, Italy) providing a controlled oxidation and reduction. Gases were separated in the helium carrier using a packed gas chromatograph (HayeSep D 80/100, Grace Davison, Australia) at room temperature and passed to a stable isotope ratio mass spectrometer (Isoprime, Micromass U.K., Manchester, U.K.). A pulse of reference CO_2 succeeded each CO_2 sample peak, to correct for pulse to pulse variation. Standards used were a C3 beet sucrose (Beet89) with a δ^{13}C of -24.62‰ Vienna Peedee Belemnite (VPDB) and ANU C4 cane sucrose with an accepted value of -10.45‰ VPDB. Each run commenced with two of each sucrose standard and proceeded with pairs of standards every 10 samples. Final corrections were made using the slope and offset derived from the two standards. Values were then converted to Δ form using

$$\Delta(‰) = \frac{\delta_a - \delta_p}{1 + \delta_p} \times 1000$$

where δ_a and δ_s are the δ^{13}C values for atmosphere (-8‰) and the sample, respectively (Farquhar et al. 1989).

Hyperspectral imaging and leaf temperature measurements

Hyperspectral measurements were taken using ASD FieldSpec 3 (Boulder, CO, USA). Photosynthetic parameters were then estimated using the Wheat Physiology Predictor at https://wheatpredictor.appf.org.au/ (Furbank et al. 2021).

Statistics

All statistics were performed using R (R Core Team 2021). Field analysis was performed using ASREML-R (Butler 2022) or the 'lme4' package (Bates et al. 2015). Multi-environment trials were analysed using the two-stage approach of Smith et al. (2001) facilitated by the use of the 'ASRtriala' package (Gezan et al. 2022). Models best fitting a trait in each trial were first constructed before combining using the Factor Analytic framework, identifying the optimal number of factors for each trait.

RESULTS

Identification of null alleles in *TaSAL* subtypes

Previously 5-7 SAL genes were identified in different wheat varieties (Mohr et al. 2022). Phylogenetic analysis of monocot SAL1 homologues showed independent duplications in both Pooideae and Panicoideae subfamilies of the Poaceae, with retention suggesting functional importance of both groups (Figure 1). We designated these as TaSAL1 (5A/B/D) and TaSAL2 (4A/7A/7D), with the 4A copy resulting from a known 4AL/7BS translocation (Devos et al. 1995). Chara cv., used herein, contained six copies across two paralogous groups: 5A/B/D and 4A/7A/7D.

Analysis of public RNA-seq based expression data revealed that TaSAL1 homeologues showed 10-fold higher expression than TaSAL2 and different developmental profiles (Supporting Information Fig. S1A) (Loudya et al. 2021). Co-expression analysis of the TaSALs revealed enrichment in distinct functional associations: TaSAL1 with sulfur metabolism (11-fold), DNA repair (15-fold), and aminoacyl-tRNA pathways (62-fold), while TaSAL2 associated with carbon (14-fold) and amino acid metabolism (37-fold), suggesting roles in photosynthesis and energy metabolism (Supporting Information Fig. S2).

Given this evidence of differential expression and coexpression, we aimed to investigate the relative impact of targeted reductions in TaSAL1 and TaSAL2. We screened a Chara HIB population (M3 generation) for single gene knockouts (Supporting Information Fig. S3). Five lines were identified, two in TaSAL1-5D (S93 and S803, designated 5D.1 and 5D.2) and three in TaSAL2-4A (S705, S959 and S280, designated 4A.1, 4A.2 and 4A.3), and systematic crosses between these lines were generated (Supporting Information Table S2).

Genomic characterisation of background deletions in the 12 lines was performed using two targeted Genotype-by-Sequencing (tGBS)

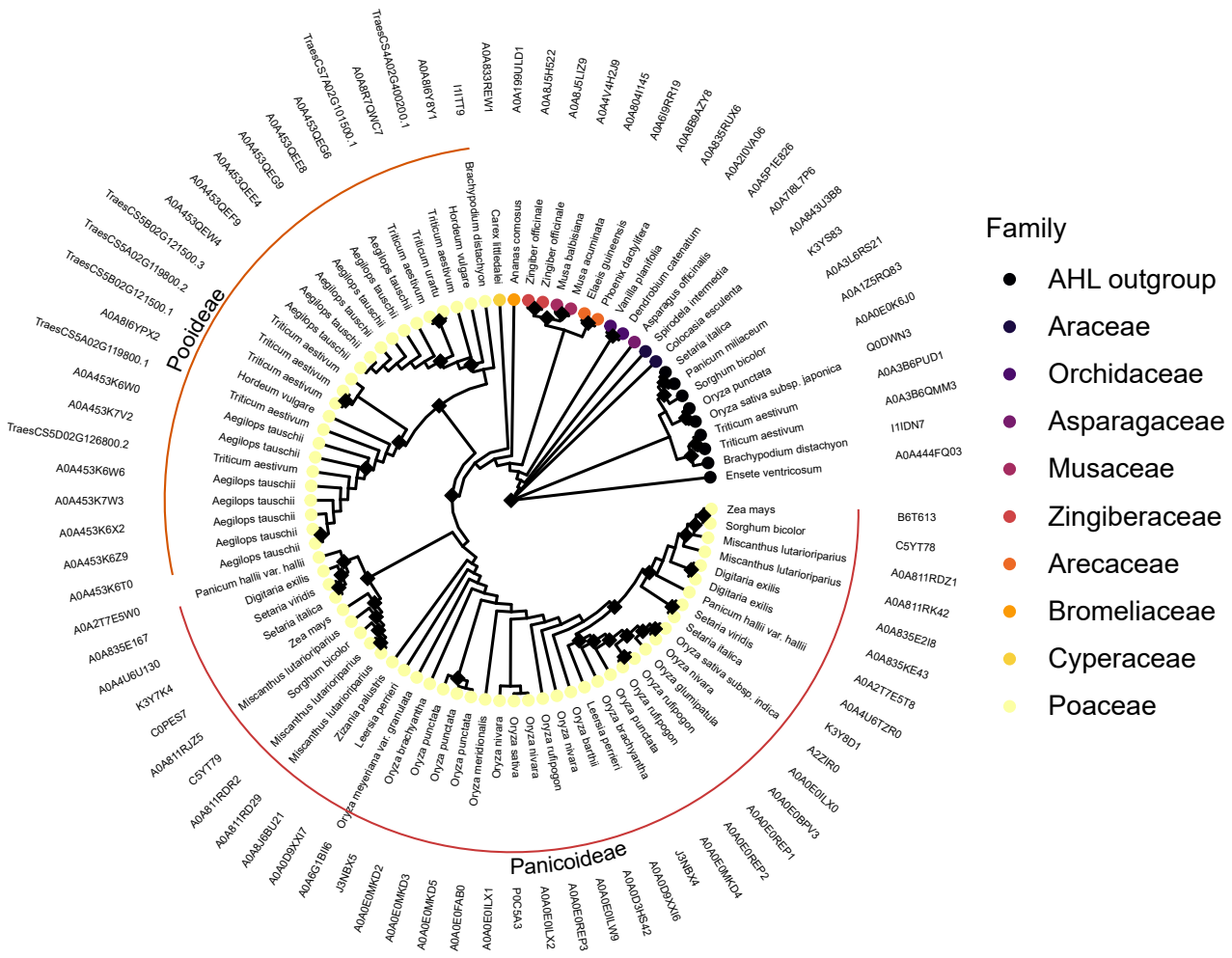

FIGURE 1 Cladogram of Liliopsida SAL1 amino acid sequences. Branch tips (sequences) are coloured according to their taxonomic ranking and labelled by species and accession including SAL1 protein family Arabidopsis haliotolerance2-like (AHL) outgroup. Nodes with black diamonds indicate branches with high confidence (ultrafast bootstrap scores > 95).

methods to genotype these lines and identify deletions. The GBSs confirmed the PCR demonstrating that all lines had complete deletions in the respective TaSAL homeologue (Supporting Information Dataset 1). The size of the deletions varied from minimal additional deletions of other loci, through to line 4A.1 (originally identified as S705), which was shown to have an additional large deletion in Chromosome 1B. Other than this line and its associated double mutants, no other incidental mutations were shown to alter traits analysed in this study.

Selective knockout of SAL genes lowers SAL activity under stress

In order to ascertain the effects of singular and combinatorial mutations in SAL subtypes on PAP concentrations and SAL enzymatic activity, they were assessed under controlled glasshouse settings with conditions of adequate water and those subjected to drought schedules (detailed in Methods). The quantification of PAP levels in wheat has not been previously reported, presenting significant challenges in this study that necessitated a year-long optimisation of our extraction and purification methodologies to remove co-eluting compounds that obscured PAP.

Under sufficient water, there was no significant difference observed in PAP levels (Supporting Information Fig. S4) or SAL activity between the mutant and control lines. However, most mutant lines showed significant decreases in SAL activity of up to 60%, compared to Chara, and several mutant lines showed increased PAP accumulation at the time of anthesis under moderate Cyclic Drought (PAP see Supporting Information Fig. S4, SAL see Figure 2). These genotype-dependent differences were confirmed for both measures (genotype:treatment interaction: PAP content $F_{(12,52)} = 2.42, p = 0.014$; SAL1 activity $F_{(12,52)} = 4.01$, $p = 0.00022$). The main effect for both PAP content and SAL activity under stress was genotype ($p < 0.001$ $F_{(12,52)} = 4.61$ and 8.56, respectively using false discovery rate correction). These results suggest that deletion of one or more TaSAL1 copies maintains basal PAP levels under unstressed conditions. There is, however, significantly lower

SAL1 activity in the TaSAL lines under drought, meaning less stress may be required to trigger PAP accumulation.

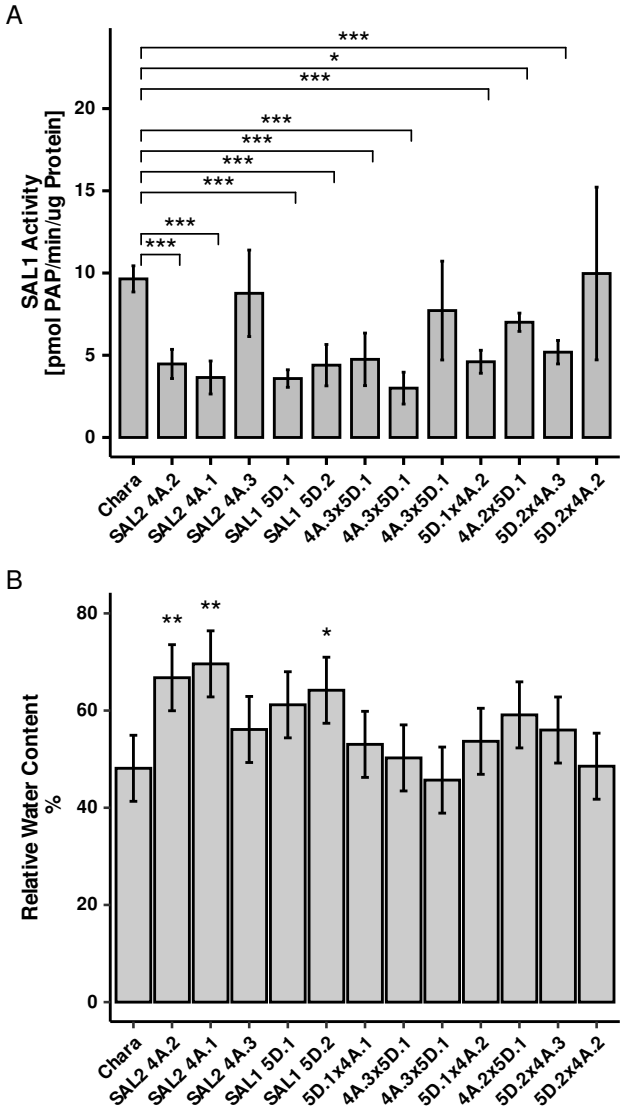

FIGURE 2 Comparison of SAL1 activity (A) and Relative water content (B) in *TaSAL1* mutant lines under Cyclic Drought stress. (A) SAL activity level of mutant lines under 21 days drought treatment. Mean ± SD. *P*-values corrected post two-way ANOVA by estimated marginal means with FDR correction to Chara; (B) Relative water content of leaf material after 21 days drought treatment. Mean ± Half least significant difference. Values from full multivariate model for repeated measures in ASREML-R LMM. See Supporting Information Fig. S5 for full analysis. $^{*}p<0.05$, $^{**}p<0.01$, $^{***}p<0.001$.

Relative water content (RWC) was measured for all 12 lines at 7, 14 and 21 days of the forementioned withholding water under the Cyclic Drought regime (Figure 2, Supporting Information Fig. S5B), and modeled using ASREML-R as a repeated measures experiment by using a uniform multivariate model. No difference was seen in any lines at 7 days, but by day 14 four of five single nulls demonstrated increased RWC compared to Chara, as did two double null lines. At 21 days, two of three 4A null lines maintained this water advantage, as did one of two 5D null lines, while the remaining lines were no longer significantly different in RWC to Chara (Figure 2).

In summary, we established that the locus-specific knockouts had largely unchanged SAL and PAP content in well-watered conditions. There was a relatively significant reduction in SAL activity, an increase in PAP, and improved RWC under water limitation in the deletion lines. Collectively, all are indicative of priming of the SAL-PAP pathway.

Physiological analysis of unstressed and stressed TaSAL germplasm

No obvious changes to crop phenological traits were identified in TaSAL germplasm. Single mutants maintained comparable biomass, plant height, and tillering. From the 3rd leaf stage, plants were grown in two different watering regimes for 35 days. The well-watered regime was to sufficiency (normalized to pot weight), while drought was enforced by the Cyclic Drought regime. Single mutant lines had comparable plant height to Chara within regimes, whereas most double mutants were reduced in stature (Supporting Information Fig. S5A). The Treatment and Genotype interaction was significant ($F_{(12,43.4)} = 2.6$, $p < 0.05$), indicating cyclic drought impact was less severe on TaSAL mutants than Chara.

To assess drought effects on photosynthesis (*A*) and stomatal conductance (g_s), we subjected four lines at the 5/6 leaf stage plants to two regimes, well-watered (control) and withholding all water for up to 42 days (Terminal Drought regime). While photosynthesis remained stable in the control regime (Figure 3, Supporting Information Fig. S6), it declined significantly in Chara after 28 days of drought. TaSAL lines maintained higher photosynthetic rates compared to Chara over the drought period ($F_{(3,11)} = 6.67$, $p = 0.008$). Stomatal conductance was also examined in the same experiment. While drought reduced g_s across all lines ($F(1,24) = 89.25$, $p < 0.0001$, $\eta^2_G = 0.53$), there were no genotype-specific differences. This maintenance of photosynthesis despite similar g_s reductions suggests improved photosynthetic capacity under water limitation in TaSAL mutants as seen in Figure 3.

The ratio of photosynthesis to water use is known as water use efficiency and was investigated given the changes in *A* and RWC. A life-time integrated measure of water use efficiency is carbon isotope discrimination. This was determined for grain collected from plants grown under Terminal Drought and control conditions, and presented as delta (Δ). Δ is calculated using the carbon isotope ratio of both the plant samples and of air (Farquhar et al. 1989), and is positive in nature; typically C3 plants have a Δ of approximately 20×10^{-3} or 20‰. Two-way ANOVA found no significant interaction between the genotypes and the water regime, but both water regime and genotype effects were significant

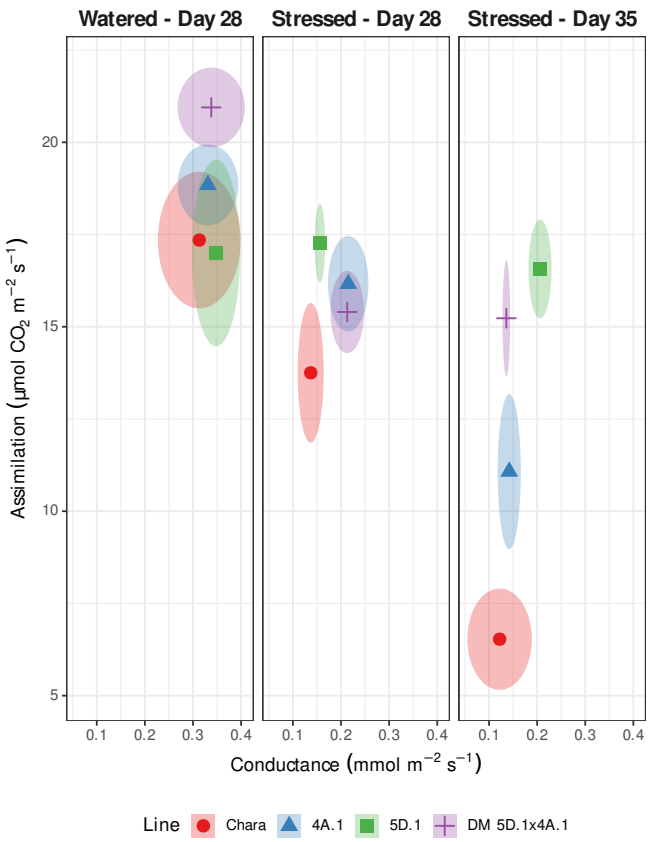

FIGURE 3 Photosynthesis and stomatal conductance days during water stress. Assimilation rate versus stomatal conductance. No differences between lines can be seen under control, watered conditions, but under water stress Assimilation rate is maintained longer in the SAL1 mutants compared to Chara control at 28 and 35 days of stress. In contrast, stomatal conductance is reduced under stressed conditions without significant differences between genotypes. Ellipses describe SE of both metrics.

and large ($F_{(1,29)}$ = 147.26, p < 0.001, η^2 = 0.84 (partial) and $F_{(5,29)}$ = 10.05, p < 0.001, η^2 = 0.63 (partial), respectively). Drought increased Δ by approximately 2.45 compared to watered control. Under both conditions, Line 4A.1 (TaSAL2 type) and a double mutant composed of line 5D.1 x 4A.1 (DM) both have significantly lower Δ than the Chara control. Additionally, under drought line 5D.2 (TaSAL1 type) also has a significantly reduced Δ (Table 1, Supporting Information Fig. S6). In summary, given the lack of difference in g_s combined with a reduction in Δ levels, we conclude improved maintenance of photosynthetic capacity in TaSAL mutants under water-limited conditions.

We then measured ABA content of leaf material under both control and Terminal Drought conditions on all single mutants to evaluate if there is any interaction between ABA and PAP (Supporting Information Fig. S7). A three-way repeated measures ANOVA was performed to evaluate the interaction of growth conditions and ABA content, using

TABLE 1 Carbon isotope discrimination (ΔC) in glasshouse conditions.

Line	ΔC Control	ΔC Drought
Chara	20.59 ± 0.12	18.43 ± 0.18
4A.1	18.77 ± 0.17***	16.39 ± 0.16***
4A.2	20.57 ± 0.84	17.78 ± 0.16
5D.1	20.02 ± 0.39	18.28 ± 0.51
5D.2	19.83 ± 0.31*	17.08 ± 0.25*
DM 5D.1x4A.1	19.29 ± 0.28***	16.43 ± 0.22***

ANOVA revealed no significance of interaction between conditions and Line; Drought increased ΔC by 2.45 (p<0.001), while Line also significantly affected ΔC (p<0.001). Lines 4A.1, 5D.2 and the double mutant 5D.1x4A.1 had significantly reduced ΔC compared to Chara control under both control and drought conditions. Mean ± SE, n=3 per Line/Condition.
Asterisks indicate significant differences from Chara: *p<0.05, **p<0.01, ***p<0.001.

paired sampling at days 0 and 28 of the experiment. There was a statistically significant three-way interaction between Genotype, Treatment and Time, ($F_{(5, 40)}$ = 3.163, p = 0.017, η_g^2 = 0.16). At 0 days, interaction of Genotype and Treatment was not significant, nor Treatment, but some significance was applied to Genotype alone (F(1, 40) = 3.71, p < 0.05); conversely, Genotype, Treatment and their interaction were all significant. Simple-simple main effects of Genotype were found to be significant under Drought, and pairwise comparison to Chara control, using a Holm correction, found all lines had significantly lower ABA content after 28 days drought. We identified that the dilution of TaSAL1 had the effect of inhibiting the ABA increase due to drought seen in the Chara control line. Of interest is the wide variance in values for Chara, implying a higher stress susceptibility compared to the single mutant lines. This observation is consistent with an hypothesis of PAP-mediated resilience limiting stress sensitivity and consequential ABA induction in the mutant lines.

In summary, plant morphology, development, and physiology were largely unaltered in unstressed conditions for single mutants. The TaSAL lines, despite only lacking 1 or 2 of the six loci, had better maintenance of plant height, enhanced photosynthesis under drought, improved RWC, and increased WUE; all in an ABA-independent manner.

Examination of retrograde signaling in field environments

Field trials were conducted at four distinct agroecological sites, Birchip, Yanco, Condobolin, and Narrabri, between 2015 and 2019 (Figure 4). The sites encompass essentially the breadth of the cereal growing regions of south-east Australia, separated by ~1,000 km. The sites have varied soil types, average rainfall (decreasing with latitude from 550 to 320 mm per year) and temperature profiles (from average monthly highs of 28.9 to 24.3°C) (Summary Tables S3 to S7). The sites were used over five years, resulting in large seasonal variation. See Methods for details on field management and trial types. Collectively, this enabled assessment in 15 different growth environments spanning years of both high

and low water availability, temperature and light. For example, actual total water availability ranged from 190 mm to 725 mm across the growing seasons; actual October average temperatures during grain fill ranged from 21 to 30 °C for highs, and establishment lows for April ranged from 6 to 14 °C (Figure 4, Supporting Information Tables S3-S7).

Field-based phenological assessments revealed no substantive changes in growth and morphology relative to the parent line, Chara. The one exception was line 4A.1 (the line with substantive off-target deletions) and its associated double mutants, which showed a shorter and spindly stature compared to Chara and the other two 4A deletion alleles, consistent with 4A.1 having more off-target lesions.

Canopy temperature reflects stomatal aperture, which PAP can directly and rapidly regulate (Pornsiriwong et al. 2017, Estavillo et al. 2011, Wilson et al. 2009). Exogenous application of PAP closes wheat and barley stomata within minutes, as rapidly as ABA (Pornsiriwong et al. 2017, Zhao et al. 2019). As a proxy for transitory and diurnal responses to SAL1-PAP signaling, we measured canopy temperatures six times over seven hours of daylight. Measures were collected at Narrabri, NSW, on two consecutive days in 2017 and once in 2019 using infrared cameras deployed on drones and helicopters.

TaSAL mutant canopy temperatures were increased compared to Chara in the middle of the day in several different lines (see Figure 5, Supporting Information Figs S9 and S10), indicating that stomata in these TaSAL lines were closed to a greater degree than the control. These trials were analysed separately as Multivariate Repeated Measures Linear Mixed Effects Models, with each plot being imaged using drone-based IR cameras at multiple times of the day. Results presented are Best Linear Unbiased Estimates (BLUEs) at each time point $\pm$ standard errors.

Both trial types in 2017 show no significant differences early or late in the day for any genotypes, indicating no constitutive alterations in stomatal aperture in the field, which is consistent with the lines being primed for stress responsiveness, and differ to prior publications in pot experiments for complete knockout/down lines (Figure 5).

In contrast, during the day there were significantly increased canopy temperatures for almost all *TaSAL* lines compared to Chara, and at multiple time points during the middle of the day (Figure 5). Both TaSAL2 group knockouts (5D.1 and 5D.2) and the 5D.1x4A.1 double null had consistent increases of up to 1.2°C, while one of two TaSAL2 knockouts also demonstrated such increases. In the 2019 trials, two lines demonstrated a significantly increased leaf temperature at 1.15 pm, lines 5D.2 and 5D.1x4A.1, more than 1.5°C higher than the Chara control (Supplementary Fig. S4). This increase was only significant in the water supplemented trial. Interestingly, 2019 ambient temperatures were much higher than in 2017 trials. The 9 am temperature measured in 2019 was approximately 19.5°C, while in 2017 it was as low as 13.5°C at 9 am on day 2 (Supporting Information Figs S8 and S9), while the maximum reached at 1.15 pm in 2019 was 27°C under irrigated conditions, and 29-31°C in the rainfed trial, compared to 19-22°C in 2017.

Photosynthesis-related traits were predicted for field grown materials using hyperspectral imaging, enabling the measurement of photosynthetic parameters at scale. Hyperspectral data was collected for the two trials at Narrabri 2019 (Supporting Information Fig. S10). Predictions of photosynthesis-related traits were produced using the Wheat Physiology Predictor (Furbank et al. 2021). This predicts leaf mass per area (LMA), nitrogen content per unit area (N_{area}) and mass (N_{mass}), maximum rate of carboxylation of photosynthesis at ambient temperature (V_{cmax}), 25°C (V_{cmax25}) and corrected for nitrogen (V_{cmax25}/N_{area}, election transport rate (J), CO_2 assimilation rate (Photo), chlorophyll content (SPAD) and stomatal conductance (g_s/Cond).

Linear mixed effects models found no changes in V_{cmax} measures in either trial, with the exception of one double null (5D.2$\times$4A.2) in rainfed conditions, and another double 4A.3$\times$5D.1 when expressed as V_{cmax25}/N_{area}. Maximum rates of carboxylation were more stable under water supplementation for those lines than rainfed, but no large differences could be identified for these traits. Leaf mass and nitrogen per unit area were increased in line 5D.2, or double nulls derived from line 5D.2 under rainfed conditions. These lines also exhibited an increased SPAD/chlorophyll content. One line, 5D.2$\times$4A.3, demonstrated a consistent increase in stomatal conductance, but no other lines exhibited this change.

Analysis of life-time integrated measures of retrograde signaling

Yield, biomass and water productivity were assessed as life-time integrated traits of plant performance, reasoning that if the effect of repeated retrograde signalling is cumulative, altered PAP responsiveness will be reflected in the alteration of these traits in different environments, compared to Chara (Figure 4).

These data were assessed by a two-stage multi-environment trial (MET) analysis of 15 trials that varied substantially for temperature, rainfall, irrigation or lack thereof, and latitude. We used a Factor Analytic approach (Gezan et al. 2022, Smith et al. 2001). As expected, variation between environments impacted yield, biomass and water productivity (individual trial BLUEs presented in Figure 6); more interestingly, yield differences between SAL genotypes and Chara exhibited considerable variability. Line 4A.2 had a range of yield differences, from an increase of over 30% in Condobolin 2017, down to a low of -7% in very hard conditions in Birchip 2018.

Predictions of yield averaged across trials found one line, 4A.2, had a significant increase in yield compared to control (approximately 4%), while its sister 4A null line, 4A.3, demonstrated an increased yield of 8%. In the integrated MET analysis this was not significant, due to the small number of trials it was included in, however in those trials it was grown, there was a statistically relevant increase when analysed as single sites (Table 2). The TaSAL1 subtype had a consistent yield penalty compared to Chara. (Table 2).

A multivariate 3rd order Factor Analytic model was used to combine these results with appropriate weighting, allowing direct prediction of

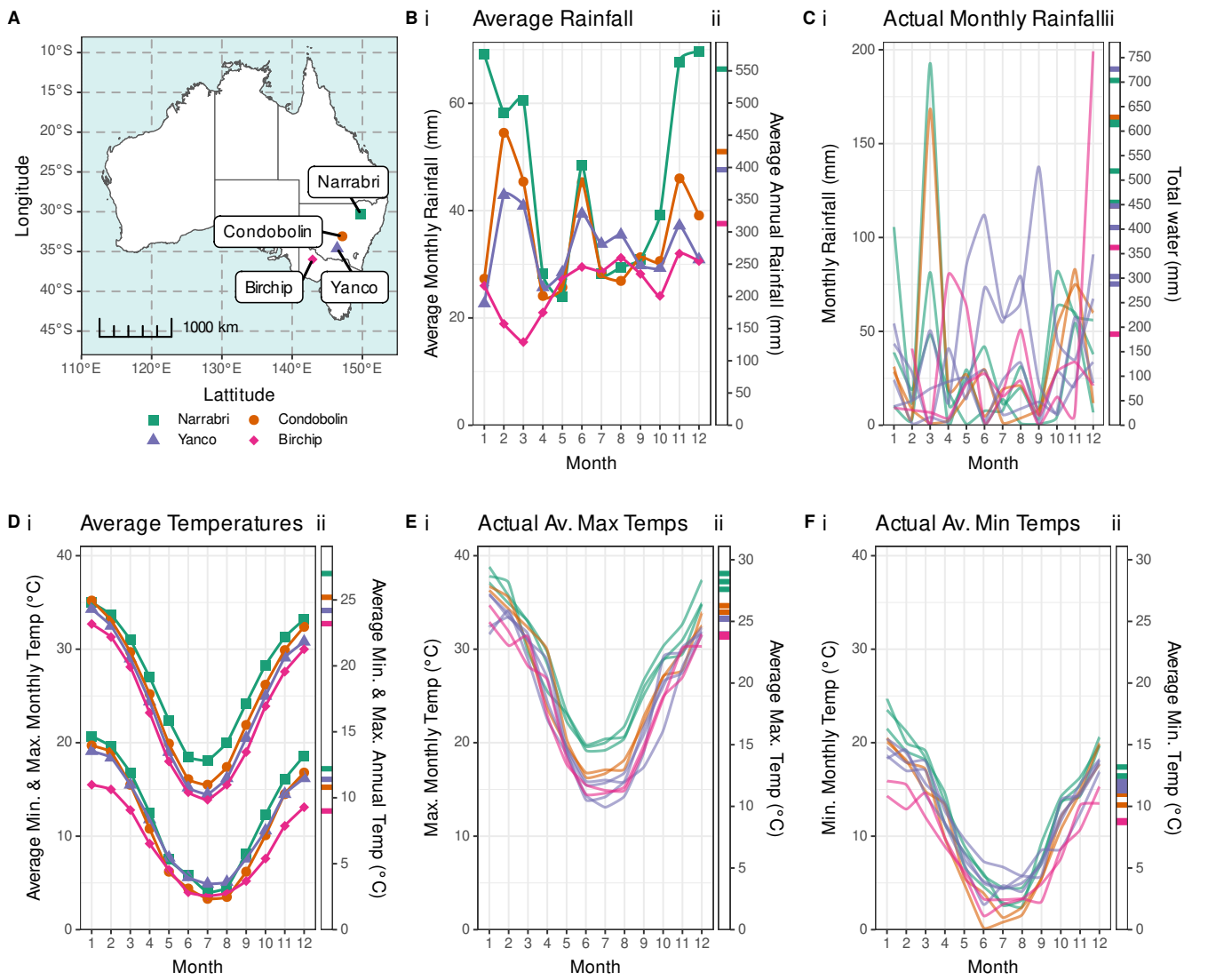

FIGURE 4 Trial environmental characteristics. *A* Map of trial locations. *B*: **i** Average monthly rainfall, and **ii**, average annual rainfall by site. *C*: **i**, Actual monthly rainfall by trial; **ii**, Total water by trial. *D*: **i**, Average min and max monthly temp, and **ii**, min and max annual temp by site. *E* and *F*: **i** Actual monthly average max and min temp (resp.) by site, and **ii**, actual yearly max and min temp (resp.) by site.

best linear unbiased predictions (BLUPs) for all lines and to predict stability of yield across sites. FA1 accounted for 90% of the variance. Together the three factors in the analytic model accounted for approximately 95% of all variance across the environments. Model biplot indicating cultivar (points) suitability to environments (arrows) and genetic covariance, indicating the magnitude of genetic variation in each environment and the degree of genetic correlation between environments, is included in Supporting Information Fig. S11. We tested the model using environmental factors, such as latitude, rainfall, irrigation, and temperature, via PCA or Random Forests and they did not explain FA1; rather, it was best explained by the genotypes.

Water productivity measures yield per unit of actual available water for a given site's growing season (kg/Ha/mm). Line 4A.2 showed higher water productivity compared to the Chara control, demonstrating its improved yield given the same availability of water (Table 2). Line 4A.3 also showed improved water productivity compared to Chara, though this improvement was not statistically significant in the MET analysis, but was for the individual sites. Again, the TASAL2 5D subtype mutants showed significantly poorer water productivity compared to the Chara control.

Biomass was also measured in select field environments. Unlike yield and water productivity, the TaSAL2 4A attenuation did not result in a significant increase in biomass. Line 5D.2 had a significant increase compared to Chara, from 9.41 ± 0.11 to 9.78 ± 0.11 t/Ha (p<0.05). The 5D.1x4A.1 double mutant was considerably smaller in biomass at 8.02

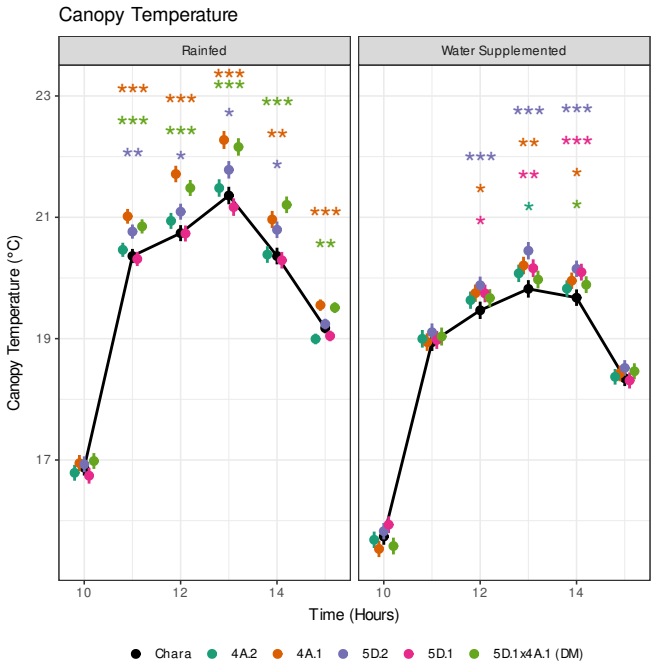

FIGURE 5 Canopy temperature in two field trials Narrabri 2017. Canopy temperature was increased compared to Chara control under both rainfed trial and water supplemented trial conditions, *$p < 0.05$, **$p < 0.01$, ***$p < 0.001$

TABLE 2 Yield, Biomass and Water Productivity Best Linear Unbiased Predictions (BLUPs).

Genotype	Trait Measurements		
	Yield (t/Ha)	Biomass (t/Ha)	Water Productivity (kg/Ha/mm Water)
Chara	4.70 ± 0.03	9.41 ± 0.11	14.20 ± 0.10
SAL2 4A.2	4.89 ± 0.03 ***	9.38 ± 0.11	14.34 ± 0.10 ***
SAL2 4A.3	5.09 ± 0.20 †	9.83 ± 0.46	14.29 ± 0.51 †
SAL1 5D.1	4.46 ± 0.03 ***	9.69 ± 0.11	13.28 ± 0.10 ***
SAL1 5D.2	4.57 ± 0.03 ***	9.78 ± 0.11 *	13.83 ± 0.10 ***
5D.1x4A.1	3.85 ± 0.03 ***	8.02 ± 0.14 ***	11.68 ± 0.10 ***

Values are from 15 trials in four locations. SAL2-type dilutions have resulted in an increase in yields compared to the control Chara variety, while the SAL1-type dilutions have resulted in reduced yields. Values are presented as predictions of random effect of genotype *pm* standard error.
Asterisks indicate significant differences from Chara: * $p < 0.05$, ** $p < 0.01$, *** $p < 0.001$.
†No significance in MET model due to low trial representation, but significant in both trials where present.

T/Ha. Overall, no patterns could be seen in biomass changes between lines and the Chara control.

Stability of yield is a measure of the variance, or lack thereof, of yield across different environments for a given genotype. It was calculated using the Superiority measure (P_i) of Lin and Binns (1988), using the mean square difference between a cultivar's yield and the maximum yield in each environment. This measure is less affected by unbalanced trials than other stability measures. The results indicated that the stability of the 4A null lines has improved compared to the Chara control, whereas the 5D lines have had a decrease in stability (Table 3). This could be indicative of a loss of capacity of the 5D lines to respond to environmental fluctuations relative to the 4A lines and Chara.

TABLE 3 Cultivar superiority (P_i) estimates for yield.

Entry	Stability (P_i)
4A.3	0.272
4A.2	0.488
Chara	0.706
5D.2	0.927
5D.1	1.087
DM - 5D.1x4A.1	2.362

Main lines investigated only included. Smaller values indicate greater stability of yield across environments.

DISCUSSION

SAL1-PAP Pathway Modulation and Plant Phenotypes

In this study we aimed to prime retrograde signal responsiveness rather than constitutively abolish/activate it. Our objectives were fourfold: first, to generate germplasm that titrates SAL1 to lower the threshold for accumulation of PAP. Second, investigate how primed PAP accumulation alters wheat phenology, stress resilience and photosynthesis. Third, we used this primed germplasm to examine roles for retrograde signaling in field environments. Fourth, we tested the hypothesis that manipulation of retrograde signaling in field conditions is manifested in relative changes to lifetime-integrated measures such as yield, biomass and water productivity.

The titration of each TaSAL homeologue set allowed examination of the pathway without previously reported constitutive phenotypes, and allowed the examination of the roles of each SAL homologue group in wheat. These groups were found to be the result of a conserved duplication that we conclude has occurred twice in the Poaceae. The conservation of the duplication in the Pooideae, distinct tissue expression and co-expression patterns, along with contrasting effects in field assessments of knockouts of TaSAL1 and TaSAL2 subtypes, are evidence towards specialization within subgroups; however, the nature of this subgrouping is far from clear as yet - be it subfunctionalisation or simply relative expression levels.

Knockouts of SAL subtypes 4A (TaSAL2 group) or 5D (TaSAL1 group) did not lower SAL activity or increase PAP in unstressed conditions, but in response to water deficit did lower relative SAL activity in most lines by up to 60% and could elevate PAP levels. The mild attenuation of SAL activity is expected to allow PAP levels to have a greater capacity to rise early in stress, and if maximal activity is reduced, peaks in PAP may be higher and more sustained. In turn, this will lead to a modified pattern

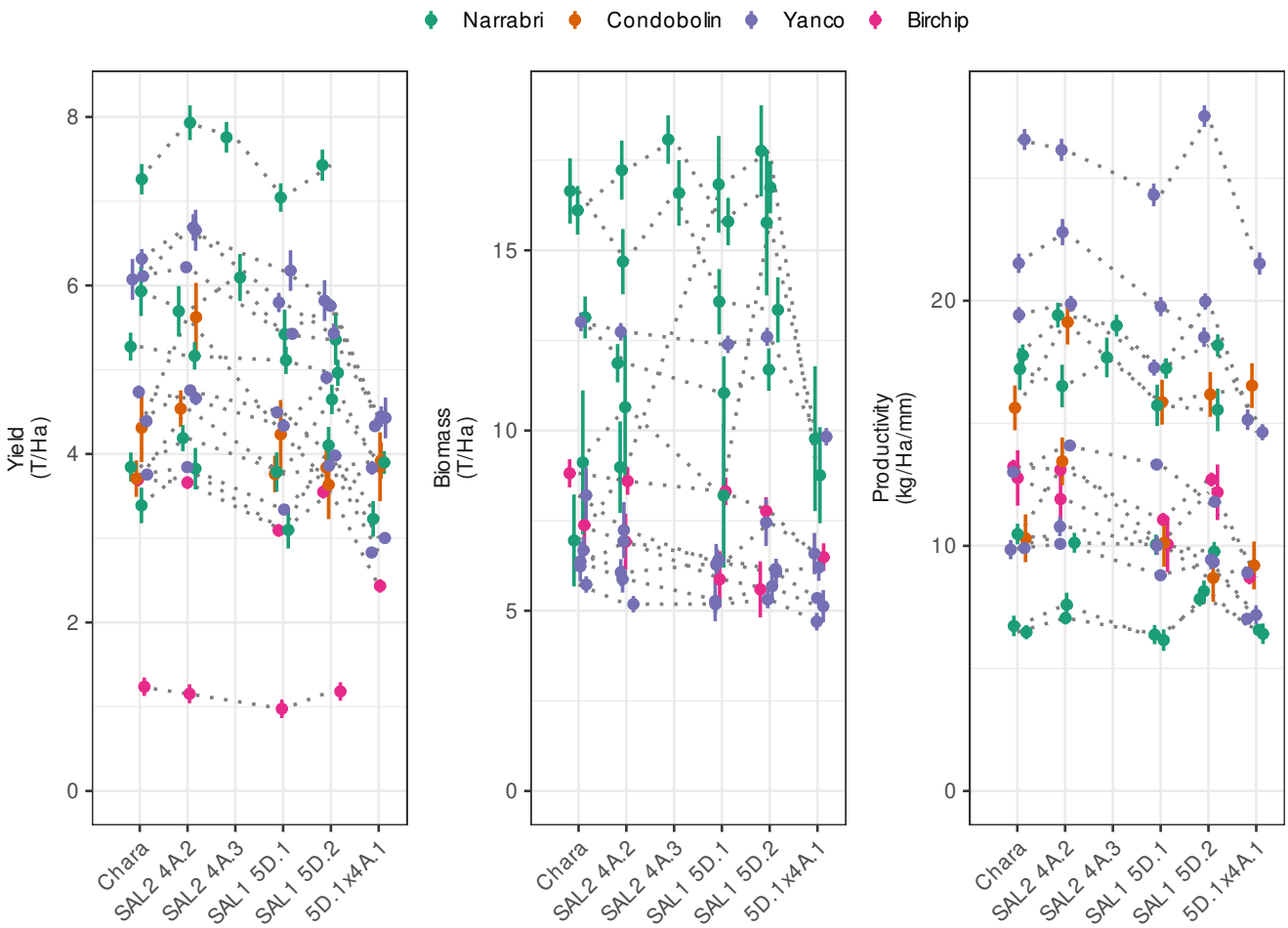

FIGURE 6 Yield characterisation of SAL1 wheat lines grown under field conditions, including yield, aboveground biomass and water productivity, in the form of Best Linear Unbiased Estimates from individual field trials. Lines 4A.2 and 4A.3 (the SAL2 form) generally demonstrate yield improvement over Chara in most trials, and an improved water productivity and increased biomass. The SAL1 type knockouts (5D lines) generally show diminished yield metrics, as does the represented double null.

of stress signals then communicated to the nucleus. What is significant is that titrating SAL activity raises PAP only under stress, thereby generating a set of lines that prime retrograde signal responsiveness.

In contrast to the *Arabidopsis sal1* knockout mutant morphology phenotypes, our wheat lines exhibited very few, if any, growth phenotypes during glasshouse evaluations (see Supporting Information Fig. S5). Under well-watered conditions, growth and tiller numbers remained mostly consistent with the Chara control, a pattern that persisted even under water deficit conditions. The height of the plant only varied marginally under well-watered conditions, and this difference was minimised under water-limiting conditions. This less severe height change is consistent with the previously reported gene editing studies that knocked out all SAL genes (Mohr et al. 2022, Abdallah et al. 2022). Modern commercial wheat cultivars have conventional Rht dwarfing genes, as does our Chara parental line (Rht-B1b, (Rebetzke et al. 2014)), many of which encode GA-insensitive DELLA proteins. Growth of such wheat cultivars is unaffected by the addition of paclobutrazol, a compound that inhibits GA biosynthesis (Tonkinson et al. 1995). Phua et al. (2018a) determined that the Arabidopsis *alx8* and *fry1-6* SAL1 mutants had approximately half the Gibberellin (GA4) of wild-type, and the addition of GA3 could partially restore growth and morphology. It is possible that these potential SAL1 based GA-related plant stature changes will not be reflected in modern wheat cultivars.

Analysis of Primed Retrograde Signaling in controlled and natural environments

In contrast to prior reports in wheat and Arabidopsis (Rossel et al. 2006, Pornsiriwong et al. 2017, Wilson et al. 2009, Abdallah et al. 2022, Mohr et al. 2022), our primed, selective knockdown lines maintained normal development while showing enhanced stress responses. The primed lines demonstrated improved water use efficiency, maintained relative water content, and sustained photosynthetic rates under

drought conditions. Most significantly, deletion of either SAL subtype enabled continued photosynthetic assimilation during water limitation - a novel finding for retrograde signaling pathways (Figure 3, Supporting Information Fig. S7). This maintenance of photosynthesis reveals the sophisticated interplay between chloroplast-mediated sensing and ABA-independent PAP regulation of stomatal function (Pornsiriwong et al. 2017), allowing dynamic rather than constitutive stress responses.

To date, whether retrograde signaling would function in plants grown in natural environments has been untested. This is opposed to another dynamic photo-oxidative stress amelioration process, nonphotochemical quenching, for which changing the kinetics of its inactivation and activation optimises photosynthesis for improved yield (Kromdijk et al. 2016). Could a similar opportunity be obtainable by priming retrograde signaling? How, though, can we measure it at scale across multi-site field-grown plots of wheat? We examined canopy temperature as a proxy for stomatal responses, as it dynamically fluctuates across a day, is measurable at scale, and responds rapidly to exogenous and endogenous PAP (Pornsiriwong et al. 2017, Zhao et al. 2019). TaSAL mutants showed increased canopy temperatures specifically during midday stress periods, with no differences in morning or evening, indicating enhanced rather than constitutive regulation (Figure 5, Supporting Information Figs S9 and S10). The temperature differences between TaSAL lines and Chara were more pronounced under rainfed versus irrigated conditions, with differences approaching 1°C. These patterns are consistent with the primed TASAL lines better dynamically regulating stomatal aperture diurnally, maximising opening under mild conditions to benefit photosynthesis and growth.

Integration of Retrograde Signaling- From Immediate Responses to Lifetime Effects

Traditionally, retrograde signaling has been studied in responses to controlled stresses, revealing regulation of oxidative stress genes over seconds to hours (Chan et al. 2010, Crawford et al. 2018). However, chloroplasts continuously sense environmental conditions, and constitutive alterations to retrograde signals - whether through SAL1 mutation or changes to other signals such as β-cyclocitral - lead to sustained developmental changes (Jiang and Dehesh 2021, Sierra et al. 2022).

Our primed TaSAL lines provided the opportunity to test the hypothesis that dynamic retrograde signaling can integrate environmental information over time to shape overall plant performance. Chara itself yielded from 1.24 T/Ha up to 7.26 T/Ha, an over 5-fold variation: an indication of the diversity of environments represented (Figure 6, Supporting Information Fig. S12). We observed considerable yield differences for the mutant lines compared to Chara between different sites, and within site variations in season and water regimes. Furthermore, the 4A and 5D loci differed from each other in their variation to Chara. For example, the TaSAL2 representative 4A.2 and 4A.3 nulls performed at or above Chara levels; 4A.2 performed over 30% better than Chara in Condobolin in the 2017 trial (4.31 compared to 5.62 T/Ha).

From the final model, 4A.2 was found across all environments to have an improved predicted yield (BLUP) of over 4%, while its sister 4A.3 was even higher at approximately 8%. With few exceptions, 4A2 lines yielded better or the same as Chara. In contrast, the TaSAL1 nulls 5D.1 and 5D.2 responded worse in most environments, consistently yielding at or below the level of Chara. Similarly, water productivity found the same pattern of TaSAL2 4A lines being better able to adapt to their environment than Chara, which was in turn better than TaSAL1 lines. Combinations of these nulls representing TaSAL1 and TaSAL2 co-modulation produced similarly mixed results to the TaSAL1 deletions, suggesting that further reductions in SAL-PAP signaling are of no advantage for successfully integrating sensing of environmental variance.

The factor analytic model revealed a striking pattern in the multi-environment trial data, with the first factor accounting for over 90% of the variation, and a cumulative 95% explained by a third-order model. The consistency of responses across diverse environments suggests these genes may influence fundamental adaptation mechanisms, rather than environment-specific responses. We propose FA1 is more reflective of genetic than environmental differences. Attempts to explain the variation in FA1 using factors that differed at the sites, such as latitude, rainfall, irrigation, and temperature, via PCA or Random Forests, were unsuccessful. Rather, FA1 at 90% is best explained by the targeted lesions in TaSAL, and not the diversity of environments or the different genetic architecture due to HIB1 lesions. Similarly, the loadings plot (Supporting Information Fig. S11) demonstrates that only the 4A.1 line is considerably unrelated in response to the environment compared to other single null lines, reflective of its unrelated off-target deletions noted above, and assures that the other deletion lines are consistent with a single gene driving this trait.

Yield stability describes how much yield varies between different environments. If altering retrograde signaling differentially affects a plant's ability to sense and respond to environmental perturbations, then yield stability should change for better or worse. Our results show a locus-dependent change in yield stability, consistent with this hypothesis; namely, the 4A locus deletion improved yield stability, while 5D locus deletions reduced it. The increase in yield stability for the TaSAL2 locus is consistent with an improved cumulative integration of transient responses to its environment.

Breaking the Yield-Resilience Trade-off

There has been a view in crop improvement that there is often an inherent trade-off between yield potential and stress resilience. Development of high-yielding varieties can introduce environmental yield penalties or instability through inadvertent selection under optimal conditions (Dietz et al. 2021). For example, lettuce breeding led to shallower root systems that perform well under irrigation but poorly in stress (Jackson 1995). In wheat, such trade-offs manifest in multiple traits including nutrition, flowering time, and architecture (Dwivedi et al. 2021). Even traits selected specifically for stress tolerance can penalize yield -

as seen with stem carbohydrate storage, which improves drought survival but reduces grain-filling efficiency in good seasons (Blum 1998, Rebetzke et al. 2008).

Our findings challenge this assumption by demonstrating that a carefully modulated stress signaling mechanism can enhance both productivity and resilience. Instead of constitutive changes leading to improved stress tolerance at the cost of growth, selective reduction of SAL activity creates a primed state with enhanced stress responsiveness. The ability to more rapidly accumulate PAP under stress conditions has not come at the cost of normal development. This is confirmed by improvements in relative water content and sustained photosynthesis under stress, coupled with improved water use efficiency through dynamic stomatal regulation demonstrated by canopy temperature patterns.

The finding of improved yield and resilience emerged from two key aspects of this study. First, the contrasting effects of TaSAL1 versus TaSAL2 deletions highlight the importance of locus targeted modification rather than complete pathway disruption. The attenuation of SAL1 by the TaSAL2 homeologous group (4A) is sufficient to elicit the improved performance, but the TaSAL1 group (5D) produces a yield penalty. Second, recent reports highlight the limited success in translating single-gene traits for yield improvement (Simmons et al. 2021, Khaipho-Burch et al. 2023), particularly where initial assessment was via controlled conditions. At the initiation of this study, the legislative requirements for GM/gene edited field trials were highly restrictive in Australia; in order to observe these TaSAL primed materials in field conditions, it was necessary to use mutation methodologies, rather than gene editing. Our evaluation under diverse field conditions revealed that TaSAL2 modifications enhanced both productivity and stability: insights that could not have emerged from controlled studies.

Conclusions

Modulating retrograde signaling in field environments results in locus-specific differences in biomass, yield, water productivity, and yield stability. The 5D locus improves resilience at the expense of yield, whereas the 4A locus results in gains in both and thus yield stability, which is an indication of better acclimation. Therefore, improving the dynamic nature of retrograde signaling, such as the priming of the SAl1-PAP pathway herein, can enhance responsiveness to multi-stress environments by maintaining photosynthesis whilst acclimating to oxidative stress and water deficits. Importantly, we have shown retrograde signaling is not just initiating a series of transient then forgotten responses, but rather integrates environmental information across a plant's lifecycle to improve yield stability and water productivity.

AUTHOR CONTRIBUTIONS

AY, GJR, GME and BJP conceived the experiment(s), MM, AY, JZ, MDM, ZP, EET, EKA, CAH and DPC conducted the experiment(s), AFB, MM and BJP analysed the results. AFB, MM, KXC and BJP wrote and reviewed the manuscript. BJP and AY share corresponding authorship. AFB, MM and AY contributed equally to this work.

ACKNOWLEDGMENTS

The authors acknowledge and thank Dr Zhongyi Li of CSIRO Agriculture and Food for access to the HIB population and for his advice. We also thank Dr Hilary Stuart-Williams of the Farquhar Laboratory and ANU's Stable Isotope Laboratory for assistance and guidance of δ^{13}C isotope discrimination analysis. We thank Professor Owen Atkin for his helpful discussion and encouragement. This work was supported by the Australian Grains Research and Development Corporation (GRDC) through grant ANU00020. AFB, MM and BJP were supported by an Australian Research Council Australian Laureate Fellowship (FL190100056). BJP, KXC and ZP are supported by the Australian Research Council Training Centre for Accelerated Future Crops Development (IC210100047).

FINANCIAL DISCLOSURE

None reported.

CONFLICT OF INTEREST

The authors declare no potential conflict of interest.

REFERENCES

Abdallah, N.A., **Elsharawy, H.**, **Abulela, H.A.**, **Thilmony, R.**, **Abdelhadi, A.A.** & **Elarabi, N.I.** (2022) Multiplex CRISPR/Cas9-mediated genome editing to address drought tolerance in wheat. *GM Crops & Food*, 16(1), 1–17. doi:10.1080/21645698.2022.2120313. URL https://www.tandfonline.com/doi/full/10.1080/21645698.2022.2120313

Ashykhmina, N., **Lorenz, M.**, **Frerigmann, H.**, **Koprivova, A.**, **Hofsetz, E.**, **Stührwohldt, N.** & **others** (2019) PAPST2 Plays Critical Roles in Removing the Stress Signaling Molecule 3′-Phosphoadenosine 5′-Phosphate from the Cytosol and Its Subsequent Degradation in Plastids and Mitochondria. *The Plant Cell*, 31(1), 231–249. doi:10.1105/tpc.18.00512. URL https://academic.oup.com/plcell/article/31/1/231-249/5974187

Bates, D., **Mächler, M.**, **Bolker, B.** & **Walker, S.** (2015) Fitting Linear Mixed-Effects Models Using lme4. *Journal of Statistical Software*, 67(1), 1–48. doi:10.18637/jss.v067.i01. URL http://www.jstatsoft.org/v67/i01/

Blum, A. (1998) Improving wheat grain filling under stress by stem reserve mobilisation. *Euphytica*, 100(1-3), 77–83. doi:10.1023/A:1018303922482. URL https://link.springer.com/article/10.1023/A:1018303922482

Bowerman, A.F., **Byrt, C.S.**, **Roy, S.J.**, **Whitney, S.M.**, **Mortimer, J.C.**, **Ankeny, R.A.** & **others** (2023) Potential abiotic stress targets for modern genetic manipulation. *The Plant Cell*, 35(1), 139–161. doi:10.1093/plcell/koac327. URL https://academic.oup.com/plcell/article/35/1/139/6827802

Bowne, J.B., **Erwin, T.A.**, **Juttner, J.**, **Schnurbusch, T.**, **Langridge, P.**, **Bacic, A.** & **others** (2012) Drought Responses of Leaf Tissues from Wheat Cultivars of Differing Drought Tolerance at the Metabolite Level. *Molecular Plant*, 5(2), 418–429. doi:10.1093/mp/ssr114. URL https://linkinghub.elsevier.com/retrieve/pii/S1674205214601295

Butler, D. (2022) *asreml: Fits the Linear Mixed Model*. R package version 4.1.0.176.

Calderon, R.H. & **Strand, Å.** (2021) How retrograde signaling is intertwined with the evolution of photosynthetic eukaryotes. *Current Opinion in Plant Biology*, 63, 102093. doi:10.1016/j.pbi.2021.102093.

URL https://linkinghub.elsevier.com/retrieve/pii/S1369526621000935

Chan, K.X., **Crisp, P.A.**, **Estavillo, G.M.** & **Pogson, B.J.** (2010) Chloroplast-to-nucleus communication. *Plant Signaling & Behavior*, 5(12), 1575–1582. doi:10.4161/psb.5.12.13758.
URL http://www.tandfonline.com/doi/abs/10.4161/psb.5.12.13758

Chan, K.X., **Mabbitt, P.D.**, **Phua, S.Y.**, **Mueller, J.W.**, **Nisar, N.**, **Gigolashvili, T.** & **others** (2016) Sensing and signaling of oxidative stress in chloroplasts by inactivation of the SAL1 phosphoadenosine phosphatase. *Proceedings of the National Academy of Sciences*, 113(31), E4567–E4576. doi:10.1073/pnas.1604936113.
URL https://pnas.org/doi/full/10.1073/pnas.1604936113

Chan, K.X., **Phua, S.Y.**, **Crisp, P.**, **McQuinn, R.** & **Pogson, B.J.** (2016) Learning the Languages of the Chloroplast: Retrograde Signaling and Beyond. *Annual Review of Plant Biology*, 67(1), 25–53. doi:10.1146/annurev-arplant-043015-111854.
URL https://www.annualreviews.org/doi/10.1146/annurev-arplant-043015-111854

Chidzanga, C., **Fleury, D.**, **Baumann, U.**, **Mullan, D.**, **Watanabe, S.**, **Kalambettu, P.** & **others** (2021) Development of an Australian Bread Wheat Nested Association Mapping Population, a New Genetic Diversity Resource for Breeding under Dry and Hot Climates. *International Journal of Molecular Sciences*, 22(9), 4348. doi:10.3390/ijms22094348.
URL https://www.mdpi.com/1422-0067/22/9/4348

Crawford, T., **Lehotai, N.** & **Strand, Å.** (2018) The role of retrograde signals during plant stress responses. *Journal of Experimental Botany*, 69(11), 2783–2795. doi:10.1093/jxb/erx481.
URL https://academic.oup.com/jxb/article/69/11/2783/4769842

Crisp, P.A., **Smith, A.B.**, **Ganguly, D.R.**, **Murray, K.D.**, **Eichten, S.R.**, **Millar, A.A.** & **others** (2018) RNA Polymerase II Read-Through Promotes Expression of Neighboring Genes in SAL1-PAP-XRN Retrograde Signaling. *Plant Physiology*, 178(4), 1614–1630. doi:10.1104/pp.18.00758.
URL https://academic.oup.com/plphys/article/178/4/1614-1630/6116736

Devos, K.M., **Dubcovsky, J.**, **Dvořák, J.**, **Chinoy, C.N.** & **Gale, M.D.** (1995) Structural evolution of wheat chromosomes 4A, 5A, and 7B and its impact on recombination. *Theoretical and Applied Genetics*, 91(2), 282–288. doi:10.1007/BF00220890.
URL http://link.springer.com/10.1007/BF00220890

Dietz, K., **Zörb, C.** & **Geilfus, C.** (2021) Drought and crop yield. *Plant Biology*, 23(6), 881–893. doi:10.1111/plb.13304.
URL https://onlinelibrary.wiley.com/doi/10.1111/plb.13304

Dwivedi, S.L., **Reynolds, M.P.** & **Ortiz, R.** (2021) Mitigating tradeoffs in plant breeding. *iScience*, 24(9), 102965. doi:10.1016/j.isci.2021.102965.
URL https://linkinghub.elsevier.com/retrieve/pii/S2589004221009330

Estavillo, G.M., **Crisp, P.A.**, **Pornsiriwong, W.**, **Wirtz, M.**, **Collinge, D.**, **Carrie, C.** & **others** (2011) Evidence for a SAL1-PAP Chloroplast Retrograde Pathway That Functions in Drought and High Light Signaling in Arabidopsis. *Plant Cell*, 23(11), 3992–4012. doi:10.1105/tpc.111.091033.

Farquhar, G.D., **Ehleringer, J.R.** & **Hubick, K.T.** (1989) Carbon Isotope Discrimination and Photosynthesis. *Annual Review of Plant Physiology and Plant Molecular Biology*, 40(1), 503–537. doi:10.1146/annurev.pp.40.060189.002443.
URL https://www.annualreviews.org/doi/10.1146/annurev.pp.40.060189.002443

Furbank, R.T., **Silva-Perez, V.**, **Evans, J.R.**, **Condon, A.G.**, **Estavillo, G.M.**, **He, W.** & **others** (2021) Wheat physiology predictor: predicting physiological traits in wheat from hyperspectral reflectance measurements using deep learning. *Plant Methods*, 17(1), 108. doi:10.1186/s13007-021-00806-6.
URL https://plantmethods.biomedcentral.com/articles/10.1186/s13007-021-00806-6

Ge, S.X., **Jung, D.** & **Yao, R.** (2020) ShinyGO: a graphical gene-set enrichment tool for animals and plants. *Bioinformatics*, 36(8), 2628–2629. doi:10.1093/bioinformatics/btz931.
URL https://academic.oup.com/bioinformatics/article/36/8/2628/5688742

Gezan, S.A., **Galli, G.** & **Murray, D.** (2022) *ASRtriala: An R package with complementary functions for single and multi-environment trial analyses*.
URL https://vsni.co.uk/free-software/asrtriala

Gigolashvili, T., **Geier, M.**, **Ashykhmina, N.**, **Frerigmann, H.**, **Wulfert, S.**, **Krueger, S.** & **others** (2012) The *Arabidopsis* Thylakoid ADP/ATP Carrier TAAC Has an Additional Role in Supplying Plastidic Phosphoadenosine 5′-Phosphosulfate to the Cytosol. *The Plant Cell*, 24(10), 4187–4204. doi:10.1105/tpc.112.101964.
URL https://academic.oup.com/plcell/article/24/10/4187-4204/6101551

Hirsch, J., **Misson, J.**, **Crisp, P.A.**, **David, P.**, **Bayle, V.**, **Estavillo, G.M.** & **others** (2011) A Novel fry1 Allele Reveals the Existence of a Mutant Phenotype Unrelated to 5′->3′ Exoribonuclease (XRN) Activities in Arabidopsis thaliana Roots. *PLoS ONE*, 6(2), e16724. doi:10.1371/journal.pone.0016724.
URL https://dx.plos.org/10.1371/journal.pone.0016724

Jackson, L.E. (1995) Root architecture in cultivated and wild lettuce (*Lactuca* spp.). *Plant, Cell & Environment*, 18(8), 885–894. doi:10.1111/j.1365-3040.1995.tb00597.x.
URL https://onlinelibrary.wiley.com/doi/10.1111/j.1365-3040.1995.tb00597.x

Jan, M.S., **Liu, Z.X.**, **Rochaix, J.D.** & **Sun, X.W.** (2022) Retrograde and anterograde signaling in the crosstalk between chloroplast and nucleus. *Frontiers in Plant Science*, 13, 24. doi:10.3389/fpls.2022.980237.

Jiang, J. & **Dehesh, K.** (2021) Plastidial retrograde modulation of light and hormonal signaling: an odyssey. *New Phytologist*, 230(3), 931–937. doi:10.1111/nph.17192.
URL https://nph.onlinelibrary.wiley.com/doi/10.1111/nph.17192

Khaipho-Burch, M., **Cooper, M.**, **Crossa, J.**, **de Leon, N.**, **Holland, J.**, **Lewis, R.** & **others** (2023) Genetic modification can improve crop yields — but stop overselling it. *Nature*, 621(7979), 470–473. doi:10.1038/d41586-023-02895-w.
URL https://www.nature.com/articles/d41586-023-02895-w

Kromdijk, J., **Głowacka, K.**, **Leonelli, L.**, **Gabilly, S.T.**, **Iwai, M.**, **Niyogi, K.K.** & **others** (2016) Improving photosynthesis and crop productivity by accelerating recovery from photoprotection. *Science*, 354(6314), 857–861. doi:10.1126/science.aai8878.
URL https://www.science.org/doi/10.1126/science.aai8878

Lin, C.S. & **Binns, M.R.** (1988) A Superiority Measure of Cultivar Performance for Cultivar × Location Data. *Canadian Journal of Plant Science*, 68(1), 193–198. doi:10.4141/cjps88-018.
URL http://www.nrcresearchpress.com/doi/10.4141/cjps88-018

Loudya, N., **Mishra, P.**, **Takahagi, K.**, **Uehara-Yamaguchi, Y.**, **Inoue, K.**, **Bogre, L.** & **others** (2021) Cellular and transcriptomic analyses reveal two-staged chloroplast biogenesis underpinning photosynthesis build-up in the wheat leaf. *Genome Biology*, 22(1), 1–30. doi:10.1186/S13059-021-02366-3.
URL https://genomebiology.biomedcentral.com/articles/10.1186/s13059-021-02366-3

Manmathan, H., **Shaner, D.**, **Snelling, J.**, **Tisserat, N.** & **Lapitan, N.** (2013) Virus-induced gene silencing of Arabidopsis thaliana gene homologues in wheat identifies genes conferring improved drought tolerance. *Journal of Experimental Botany*, 64(5), 1381–1392. doi:10.1093/jxb/ert003.
URL https://academic.oup.com/jxb/article-lookup/doi/10.1093/jxb/ert003

Mohr, T., **Horstman, J.**, **Gu, Y.Q.**, **Elarabi, N.I.**, **Abdallah, N.A.** & **Thilmony, R.** (2022) CRISPR-Cas9 Gene Editing of the Sal1 Gene Family in Wheat. *Plants*, 11(17), 2259. doi:10.3390/plants11172259.
URL https://www.mdpi.com/2223-7747/11/17/2259

Passioura, J.B. (2006) Viewpoint: The perils of pot experiments. *Functional Plant Biology*, 33(12), 1075. doi:10.1071/FP06223.
URL http://www.publish.csiro.au/?paper=FP06223

Phua, S.Y., **Pornsiriwong, W.**, **Chan, K.X.**, **Estavillo, G.M.** & **Pogson, B.J.** (2018) Development of strategies for genetic manipulation and fine-tuning of a chloroplast retrograde signal 3′-phosphoadenosine 5′-phosphate. *Plant Direct*, 2(1), 15. doi:10.1002/pld3.31.
URL https://onlinelibrary.wiley.com/doi/10.1002/pld3.31

Phua, S.Y., **Yan, D.W.**, **Chan, K.X.**, **Estavillo, G.M.**, **Nambara, E.** & **Pogson, B.J.** (2018) The Arabidopsis SAL1-PAP Pathway: A Case Study for Integrating Chloroplast Retrograde, Light and Hormonal Signaling in Modulating Plant Growth and Development? *Frontiers in Plant Science*, 9, 8. doi:10.3389/fpls.2018.01171.
URL https://www.frontiersin.org/journals/plant-science/articles/10.3389/fpls.2018.01171

Pogson, B.J., **Woo, N.S.**, **Förster, B.** & **Small, I.D.** (2008) Plastid signalling to the nucleus and beyond. *Trends in Plant Science*, 13(11), 602–609. doi:10.1016/j.tplants.2008.08.008.
URL https://linkinghub.elsevier.com/retrieve/pii/S1360138508002276

Pornsiriwong, W., **Estavillo, G.M.**, **Chan, K.X.**, **Tee, E.E.**, **Ganguly, D.**, **Crisp, P.A.** & **others** (2017) A chloroplast retrograde signal, 3'-phosphoadenosine 5'-phosphate, acts as a secondary messenger in abscisic acid signaling in stomatal closure and germination. *eLife*, 6, 34. doi:10.7554/eLife.23361.
URL https://elifesciences.org/articles/23361

R Core Team (2021) *R: A Language and Environment for Statistical Computing*.
URL https://www.R-project.org/

Rebetzke, G.J., **Chenu, K.**, **Biddulph, B.**, **Moeller, C.**, **Deery, D.M.**, **Rattey, A.R.** & **others** (2013) A multisite managed environment facility for targeted trait and germplasm phenotyping. *Functional Plant Biology*, 40(1), 1. doi:10.1071/FP12180.
URL http://www.publish.csiro.au/?paper=FP12180

Rebetzke, G.J., **Van Herwaarden, A.F.**, **Jenkins, C.**, **Weiss, M.**, **Lewis, D.**, **Ruuska, S.** & **others** (2008) Quantitative trait loci for water-soluble carbohydrates and associations with agronomic traits in wheat. *Australian Journal of Agricultural Research*, 59(10), 891–905. doi:10.1071/AR08067.
URL https://www.publish.csiro.au/ar/AR08067

Rebetzke, G.J., **Verbyla, A.P.**, **Verbyla, K.L.**, **Morell, M.K.** & **Cavanagh, C.R.** (2014) Use of a large multiparent wheat mapping population in genomic dissection of coleoptile and seedling growth. *Plant Biotechnology Journal*, 12(2), 219–230. doi:10.1111/pbi.12130.
URL https://onlinelibrary.wiley.com/doi/10.1111/pbi.12130

Regina, A., **Berbezy, P.**, **Kosar-Hashemi, B.**, **Li, S.**, **Cmiel, M.**, **Larroque, O.** & **others** (2015) A genetic strategy generating wheat with very high amylose content. *Plant Biotechnology Journal*, 13(9), 1276–1286. doi:10.1111/pbi.12345.
URL https://onlinelibrary.wiley.com/doi/10.1111/pbi.12345

Rossel, J.B., **Walter, P.B.**, **Hendrickson, L.**, **Chow, W.S.**, **Poole, A.**, **Mullineaux, P.M.** & **others** (2006) A mutation affecting *ASCORBATE PEROXIDASE 2* gene expression reveals a link between responses to high light and drought tolerance. *Plant, Cell & Environment*, 29(2), 269–281. doi:10.1111/j.1365-3040.2005.01419.x.
URL https://onlinelibrary.wiley.com/doi/10.1111/j.1365-3040.2005.01419.x

Sharma, D.L., **Bhoite, R.**, **Reeves, K.**, **Forrest, K.**, **Smith, R.** & **Dowla, M.A.N.N.U.** (2022) Genome-wide superior alleles, haplotypes and candidate genes associated with tolerance on sodic-dispersive soils in wheat (*Triticum aestivum* L.). *Theoretical and Applied Genetics*, 135(3), 1113–1128. doi:10.1007/s00122-021-04021-8.
URL https://link.springer.com/10.1007/s00122-021-04021-8

Sierra, J., **McQuinn, R.P.** & **Leon, P.** (2022) The role of carotenoids as a source of retrograde signals: impact on plant development and stress responses. *Journal of Experimental Botany*, 73(21), 7139–7154. doi:10.1093/JXB/ERAC292.
URL https://dx.doi.org/10.1093/jxb/erac292

Simmons, C.R., **Lafitte, H.R.**, **Reimann, K.S.**, **Brugière, N.**, **Roesler, K.**, **Albertsen, M.C.** & **others** (2021) Successes and insights of an industry biotech program to enhance maize agronomic traits. *Plant Science*, 307, 110899. doi:10.1016/j.plantsci.2021.110899.
URL https://linkinghub.elsevier.com/retrieve/pii/S0168945221000923

Smith, A., **Cullis, B.** & **Gilmour, A.** (2001) Applications: The Analysis of Crop Variety Evaluation Data in Australia. *Australian & New Zealand Journal of Statistics*, 43(2), 129–145. doi:10.1111/1467-842X.00163.
URL https://onlinelibrary.wiley.com/doi/10.1111/1467-842X.00163

Tonkinson, C.L., **Lyndon, R.F.**, **Arnold, G.M.** & **Lenton, J.R.** (1995) Effect of the Rht3 dwarfing gene on dynamics of cell extension in wheat leaves, and its modification by gibberellic acid and paclobutrazol. *Journal of Experimental Botany*, 46(9), 1085–1092. doi:10.1093/JXB/46.9.1085.
URL https://dx.doi.org/10.1093/jxb/46.9.1085

Wilson, P.B., **Estavillo, G.M.**, **Field, K.J.**, **Pornsiriwong, W.**, **Carroll, A.J.**, **Howell, K.A.** & **others** (2009) The nucleotidase/phosphatase SAL1 is a negative regulator of drought tolerance in Arabidopsis. *The Plant Journal*, 58(2), 299–317. doi:10.1111/j.1365-313X.2008.03780.x.
URL https://onlinelibrary.wiley.com/doi/10.1111/j.1365-313X.2008.03780.x

Zandalinas, S.I. & **Mittler, R.** (2022) Plant responses to multifactorial stress combination. *New Phytologist*, 234(4), 1161–1167. doi:10.1111/nph.18087.
URL https://nph.onlinelibrary.wiley.com/doi/10.1111/nph.18087

Zhang, H., **Zhang, F.**, **Yu, Y.**, **Feng, L.**, **Jia, J.**, **Liu, B.** & **others** (2020) A Comprehensive Online Database for Exploring ∼20,000 Public *Arabidopsis* RNA-Seq Libraries. *Molecular Plant*, 13(9), 1231–1233. doi:10.1016/j.molp.2020.08.001.
URL https://linkinghub.elsevier.com/retrieve/pii/S1674205220302574

Zhao, C., **Wang, Y.**, **Chan, K.X.**, **Marchant, D.B.**, **Franks, P.J.**, **Randall, D.** & **others** (2019) Evolution of chloroplast retrograde signaling facilitates green plant adaptation to land. *Proceedings of the National Academy of Sciences*, 116(11), 5015–5020. doi:10.1073/pnas.1812092116.
URL https://pnas.org/doi/full/10.1073/pnas.1812092116

SUPPORTING INFORMATION

Additional supporting information may be found in the online version of the article at the publisher's website.

Dataset 1 Genotype-by-sequencing results for all mutants in study.

Fig. S1 Comparison of total SAL and individual homeoforms expression levels in wheat, and variation in expression across developing seedling leaves.

Fig. S2 KEGG Pathways of co-expressed genes of TaSAL1 and TaSAL2 homologue sets.

Fig. S3 Representative agarose gel of screening for TaSAL1 mutants via PCR.

Fig. S4 PAP content under irrigated and drought conditions in glasshouse experiments.

Fig. S5 Plant height and relative water content under drought.

Fig. S6 Photosynthesis, stomatal conductance, and carbon isotope discrimination in glasshouse materials.

Fig. S7 ABA content of glasshouse-grown wheat material under Control and Drought conditions.

Fig. S8 Leaf/canopy temperature results from Narrabri 2019.

Fig. S9 Leaf/canopy temperature results from Narrabri 2017.

Fig. S10 Hyperspectral-derived estimates of photosynthesis related traits.

Fig. S11 Factor analytic model visualization of multi-environment trial analysis - Biplot and Genetic Covariance Matrix heatmap.

Table S1 Table of primers used in discovery of *TaSal1* null lines from HIB population.

Table S2 Line identifiers and *TaSal1* gene knockout.

Table S3 Narrabri environmental characteristics for all years of trials.

Table S4 Condobolin environmental characteristics for all years of trials.

Table S5 Yanco environmental characteristics for all years of trials.

Table S6 Birchip environmental characteristics for all years of trials.

Table S7 Characterising average and actual water conditions per site and year, including irrigation where used.

Table S8 Yield, Biomass and Water Productivity Best Linear Unbiased Predictions for all trials.

Method S1 Phylogenetic analysis.

Method S2 PAP extraction, preparation, and quantification by HPLC.